EXPERIMENTAL VALIDATION OF NEUTRAL BEAM CURRENT DRIVE SIMULATIONS IN TJ-II PLASMAS

S. MULAS
Laboratorio Nacional de Fusión, CIEMAT
Madrid, Spain
Email: sadig.mulas@ciemat.es

Á. CAPPA, D. LÓPEZ-BRUNA, J.L. VELASCO, I. CALVO, T. ESTRADA and TJ-II TEAM
Laboratorio Nacional de Fusión, CIEMAT
Madrid, Spain

J. KONTULA and T. KURKI-SUONIO
Aalto University
Espoo, Finland

F. PARRA
Rudolf Peierls Centre for Theoretical Physics, University of Oxford
Oxford, United Kingdom

M.J. MANTSINEN
BSC, ICREA
Barcelona, Spain

Abstract

The goal of the work is to carry out a validation of neutral beam current drive (NBCD) simulations in the TJ-II stellarator. NBCD has been estimated for NBI plasmas (without ECRH) using the Monte Carlo orbit following code ASCOT in order to determine first the fast-ion current. Then, the correction to the fast-ion current caused by the electron return current has been calculated analytically. The total plasma current measured in several NBI-heated discharges is compared to the predicted values that are obtained by adding both bootstrap current and NBCD contributions. Because of the short pulse length of NBI shots, the experimental plasma current needs to be extrapolated for times longer than the shot duration. It is shown that the theoretical value is always much higher than the measured one. The possible reasons that could explain the discrepancies are discussed.

1. INTRODUCTION

Validation of beam-driven Alfvén Eigenmodes (AEs) simulations against experimental results in fusion devices requires, among other inputs, knowing the value of the rotational-transform profile of the plasma equilibrium, which in stellarators is strongly affected by non-inductive plasma currents. Besides its importance for the interpretation of AEs experiments, which has been the initial drive for NBCD studies in TJ-II, a validation of NBI current-drive simulations in non-axisymmetric configurations is also desirable for devices that rely on precise current control. In the TJ-II stellarator, since many of the experiments were carried out with non-balanced neutral-beam injection and no measurements of the rotational transform profile are available (or present a large error in those few cases where it has been measured using MSE diagnostic [1]), a theoretical estimation of the current driven by the injection of the neutral beam (NBCD) is mandatory in order to reconstruct the equilibrium. The beam-driven current is the combination of two different contributions: the current of the fast ions and the response of the plasma electrons that tends to shield this current. The current associated with the slowing down distribution of fast ions has been obtained using the Monte Carlo orbit-following code ASCOT [2] and the return or shielding current of the electrons has been determined using the expressions derived in [3]. In general, the measured current does not reach a stable value during the shot because the current relaxation-time or L/R time (τ_{LR}) is often longer than the typical TJ-II NBI pulse duration ($\sim$100 ms) and, therefore, the validation of the theoretical results needs an estimation of the stable current that would be achieved with longer pulses. An exponential fit to the measured current evolution is used to that end [4-6]. A drawback of the simulations carried out to date is that the version of the ASCOT code used here does

not include charge-exchange (CX) processes. In devices with higher temperatures and higher NBI energies, CX losses are lower due to the strong decrease of the CX cross section. However, in the case of TJ-II NBI plasmas, in particular if they are relevant from the point of view of AEs studies, the density of neutrals in the plasma produces high CX losses and they need to be included if a reliable estimation of NBI heating is desired. In low-density conditions, guiding-center calculations with FAFNER [7] show that CX losses can reach up to 30% of the port-through power, which represents almost 70% of the available power due to the high level of shine through. The impact of disregarding CX losses in NBCD calculations in TJ-II is still an open issue that needs to be clarified.

2. EXPERIMENTAL RESULTS

The NBI system of the TJ-II stellarator consists of two (co- and counter-) tangential beams injecting 700 kW of maximum power each with a maximum energy E_{beam} = 34 keV [8]. In order to carry out a validation of the beam-driven current against the experiment, several NBI-heated plasmas with different densities have been chosen from the TJ-II database. They all exhibit approximately stationary electron line-density and temperature during the NBI phase. This should guarantee that the source of driven current is roughly constant and that the time evolution of plasma current measured experimentally is only originated by the current decay due to TJ-II plasma inductance and resistivity. In all cases, ECRH is used to only start-up and build the NBI target plasma. Figure 1 shows the time evolution of the plasma parameters and the heating power for two representative shots (P_{NBI}=430 kW and P_{NBI}=380 kW).

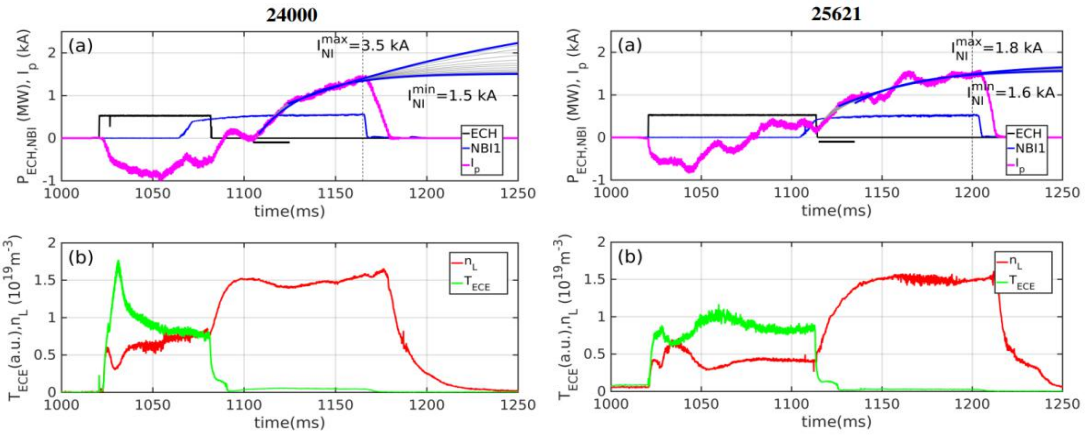

FIG. 1: (a) Time evolution of ECR and NBI heating powers and total plasma current measured by an inner Rogowski coil for shots #24000 and #25621. The result of the exponential fits obtained by following the procedure described in the text is shown in grey dashed lines together with the maximum and minimum values of the asymptotic currents (blue solid lines). The horizontal black solid line below the x-axis indicates the range of initial times taken to carry out the exponential fit and the vertical dotted line corresponds to the final time, always close to the end of the NBI pulse. (b) Time traces of electron line-density and central ECE temperature.

During the ECRH phase, provided that no EC current is being driven, the only source of current in the plasma is the bootstrap current, which is produced by the gradients of the pressure profiles. After switching on the NBI, the ECRH is switched off (see Fig. 1) and the plasma current starts evolving towards its asymptotic steady-state value. The time behaviour of the plasma current, that usually exhibits slow oscillations of the order of 0.2-0.3 kA, is the main source of error in the analysis. Taking into account that the relaxation time is comparable to the pulse duration and that the stabilization of the plasma current (I_p) takes place after several relaxation times, an exponential fit to the time trace of the measured plasma current is needed to determine the non-inductive current source. The expression of the fitting function is the following,

$$I_p(t) = I_0 e^{-t/\tau_{LR}} + I_{NI}$$

In this expression, the limit of the plasma current when $t \to \infty$ is I_{NI}, which accounts for all the different non-inductive currents in the NBI plasma: bootstrap current and NBCD. This value shall be compared with the results from the simulations. The fit result depends on the selected time interval of the plasma current since its

evolution, even after ECRH switch-off, differs from an ideal exponential. The final time is fixed at the end of the NBI pulse and a range of initial values spanning 20 ms is explored in an attempt to determine the uncertainty of the fitting procedure. The experimental value of the non-inductive current is defined as the average of the different values of I_{NI} for all the fitted time intervals and its error bar is given by the standard deviation. The results of the analysis are given in Table 1.

Stable-density NBI-plasmas are difficult to achieve in TJ-II. Only right after an optimum lithium wall conditioning, the line density can be kept constant enough so as to ensure that the evolution of the plasma current has an electrodynamic origin. Changes in the plasma profiles, that are reflected in the slowly-increasing line density, make the evolution of the plasma current deviate from an exponential and thus fitting the current is no longer an option. This is clearly visible in Fig. 2, where the evolution of the plasma current in a shot with counter-injection (NBI 2) appears to be almost linear instead of exponential. Everything considered, the number of suitable shots for NBCD studies is rather low and, out of those, only a few present a time evolution that can be approximated by an exponential curve.

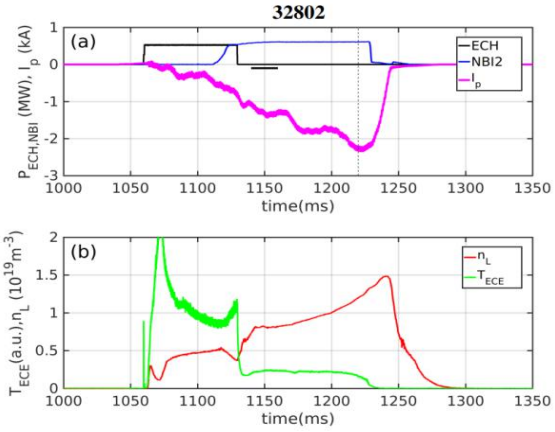

FIG. 2: (a) Time evolution of ECR and NBI heating powers and total plasma current of shot #32802. (b) Time traces of electron line-density and central ECE temperature. The plasma current does not evolve exponentially but linearly due to unstable plasma-density.

3. NBI SIMULATIONS USING ASCOT

3.1. Simulation set up

The full injection geometry of both beams, the plasma profiles and the vacuum equilibrium calculated with VMEC have been included in the BBNBI code [9] in order to simulate the ionization of the NBI-neutrals and subsequently obtain the distribution of initial markers.

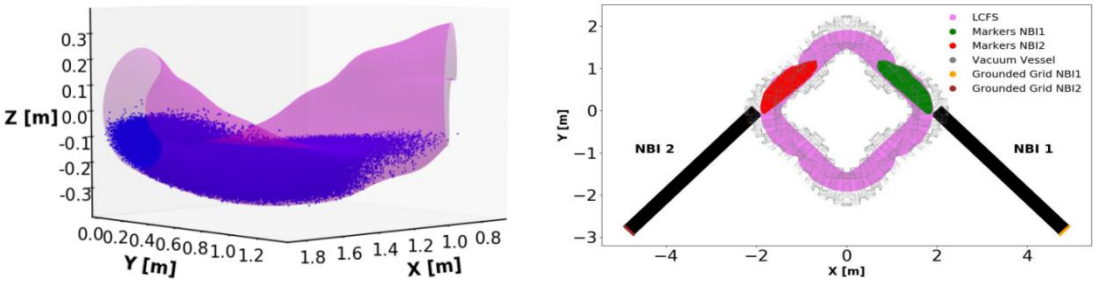

FIG. 3: Left: a 3D illustration of the ionization position of the co-injected initial markers representing beam particles and the last closed flux surface. Right: top view of the simulated neutral beams of TJ-II.

ASCOT follows the markers, integrating numerically their collisional trajectories, until each marker either slows down to twice the ion temperature at markers' location, becoming part of the thermal bulk, or hits the first wall of the device. In Fig. 3, the cloud of initial markers within the plasma is shown for both injectors.

3.2. Results

The plasma profiles used in the simulations, that have been fitted to the experimental Thomson scattering profiles, are shown in Fig. 4 and Fig. 5. In the two shots considered, the peak electron densities are $1.6 \cdot 10^{19}$, $2.5 \cdot 10^{19}$ m^3 and the peak electron temperatures 317, 250 eV respectively. The ion-temperature profiles have been chosen under the assumption that its shape is similar to the electron temperatures [10] with a peak value of 100 eV at the center of the plasma. The hydrogen-density profiles are calculated from the electron-density ones considering a flat profile of Z_{eff}=1.5 and boron (Z=5) as the only impurity.

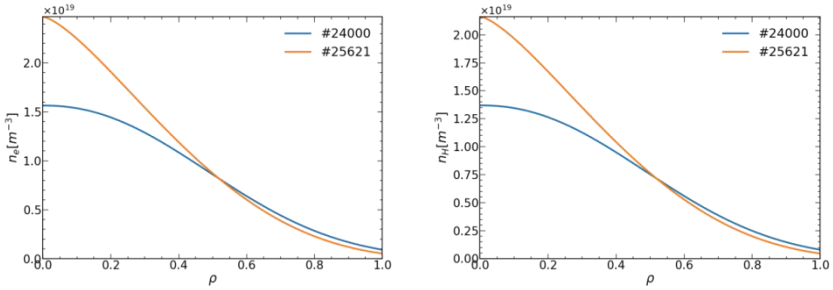

FIG. 4: Electron (left) and ion (right) density profiles of the simulated shots.

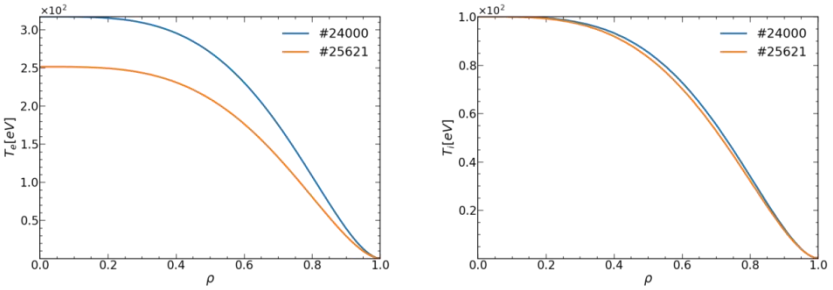

FIG. 5: Electron (left) and ion (right) temperatures profiles of the simulated shots.

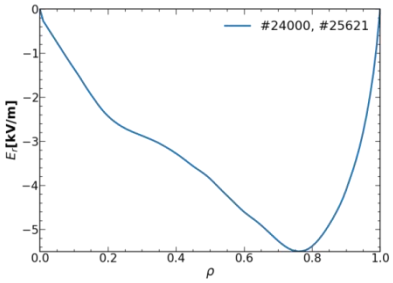

FIG. 6: Radial electric-fields used for the simulations of shots #24000 and #25621

Due to the weak influence of the electric field on the fast-ion distribution-function, a single radial electric-field profile, consistent with measurements obtained with Doppler reflectometry for shots with similar plasma parameters [11][12], has been taken in all the simulations. The profile, shown in Fig. 6, is negative, which is a characteristic of the so-called ion-root phase of the plasma during NBI injection. The slowing-down process of the injected beam ions has been simulated with ASCOT in order to obtain the steady-state distribution-function. The results of the simulations are depicted in Fig. 7. The left panel shows the steady-state distribution-function for shot #24000 in terms of parallel velocity and a radial coordinate defined here as $\rho = \sqrt{\psi}$, where ψ is the normalized toroidal-flux, while the right panel shows the parallel-velocity distribution. The co-injection of NBI1 can be noted by the fact that most of the particles have positive parallel velocities (right panel). The three steps created by the three different injection energies (E_{max}, $E_{max}/2$, $E_{max}/3$) are visible in both plots.

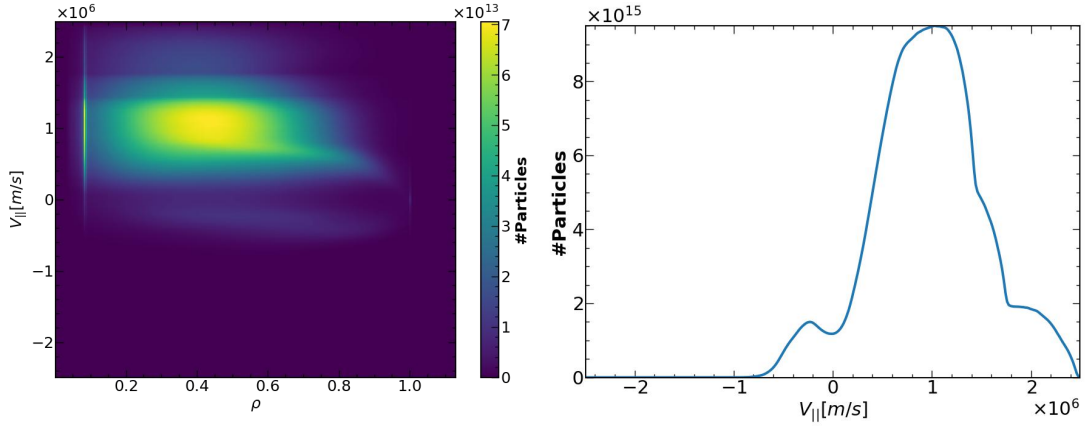

FIG. 7: Left: 2D distribution function in (ρ, $V_\parallel$)-phase space of discharge #24000. Right: parallel-velocity distributions obtained with ASCOT.

4. NEUTRAL BEAM CURRENT DRIVE

As it was mentioned in the introduction, the total current driven by the beam ($J_\parallel^{NBCD}$) is calculated as the sum of two contributions: the current carried by the fast ions ($J_{b\parallel}$) and the electron return current, which is obtained by solving the drift kinetic equation in the low-collisionality regime for $\nu_{T_e} \gg \nu_b$ where ν_b is the typical speed of the fast ions and ν_{T_e} the thermal speed of the electrons. The net current is then written as [3]

$$J_\parallel^{NBCD} = J_{b\parallel}(1 - A_s) = e n_b Z_b V_{b\parallel}(1 - A_s) \ , \tag{1}$$

where n_b is the steady-state fast-ion density and $V_{b\parallel}$ the average parallel velocity of the fast ions with charge eZ_b. The "shielding" or electron return current factor A_s is given by

$$A_s = \frac{Z_b}{Z_{eff}} \frac{B\langle B\rangle}{\langle B^2\rangle} f_c \left[1 - \frac{8}{3\sqrt{\pi}} \frac{I_1}{\left(1 + Z_{eff} + \frac{I_2 f_c}{I_3 f_t}\right)} \right] , \tag{2}$$

where

$$f_c = \frac{3}{4}\langle B^2\rangle \int_0^{1/B_{MAX}} \frac{\lambda}{\langle\sqrt{1-\lambda B}\rangle} d\lambda \ . \tag{3}$$

In equation (3), $\langle ... \rangle$ stands for the flux surface average, $f_t = 1 - f_c$ and f_c is defined as an integral over circulating (non-trapped) particles, where $\lambda \equiv \mu/E = B^{-1}\left(1 - v_\parallel^2/v^2\right)$. The integrals $I_1(Z_{eff})$, $I_2(Z_{eff})$ and I_3 in equation (3) are the following:

$$\begin{aligned} I_1 &= \int_0^\infty \frac{x^4 h(x) e^{-x^2}}{h(x) + Z_{eff}} dx \ , \\ I_2 &= \int_0^\infty \frac{x h(x) e^{-x^2}}{h(x) + Z_{eff}} dx \ , \\ I_3 &= \int_0^\infty x h(x) e^{-x^2} dx \ \approx 0.27, \end{aligned} \tag{4}$$

and $h(x)$ is given in terms of well-known special functions,

$$h(x) \equiv \Phi(x) - G(x) \ ,$$

$$\Phi(x) = \int_0^x e^{-y^2} dy \ , \tag{5}$$

$$G(x) = \frac{\Phi(x) - x\Phi'(x)}{2x^2} \ .$$

Thus, the fast-ion current is more or less efficiently shielded by the electrons depending on the value of A_s. The larger A_s, the larger the shielding current. In principle, equation (2) allows for variations on a given flux surface through its dependence on B, which is non-constant on the flux surface. In this case, since the result for n_b and $V_{b\|}$ given by ASCOT are both flux functions, we will use the flux-surface average of the shielding factor in equation (1), i.e. $\langle J_{\|}^{NBCD} \rangle = J_{b\|}(1 - \langle A_s \rangle)$, to calculate the flux-surface average of the beam current drive. Using the VMEC equilibrium of the TJ-II standard magnetic configuration and Z_{eff} values between 1.0 and 1.8 we arrive at the result shown in Fig. 8. This result shows that electron shielding is more efficient in the core plasma, where the fraction of trapped electrons is lower, and that cleaner plasmas show lower NBCD.

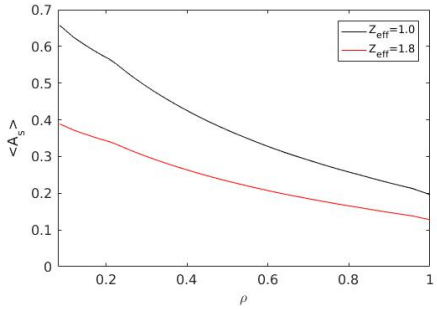

FIG. 8: Shielding factor for the TJ-II standard configuration and two values of Z_{eff}.

Using the result presented in Fig. 8 and the result for $\langle J_{b\|} \rangle$ calculated with ASCOT we can obtain the total parallel-current density driven by the neutral beam. The result is presented in Fig. 9, where the NBCD current density profile (dashed line) and the integrated current profile (solid) for discharge #24000 is presented. In this case, the total amount of NBCD present in the plasma column is 8,3 kA.

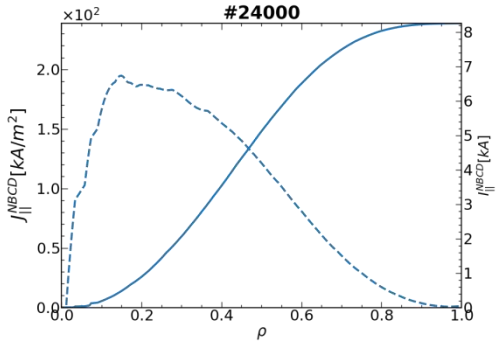

FIG. 9: Current density profiles, as calculated by eq. (1), in dashed lines and integrated current profiles (solid line) as a function of ρ.

5. COMPARISON WITH EXPERIMENTAL RESULTS

With the aim of comparing the computational results with the experimental ones, the bootstrap current must be calculated. In Fig. 10, the bootstrap current density (blue) and integrated one (red) are shown as calculated with DKES [13]. In Table 1, the values of the different current contributions integrated up to the plasma edge are shown together with the experimental measurement. The computed values of the NBCD (I_{NBCD}) correspond to

the simulated profiles of Figs. 4, 5 and 6. The error of I_{NBCD} associated with the error of the measurements of the experimental kinetic profiles, from which the fitted profiles have been obtained, is 22%. This number is the standard deviation of several NBCD values from simulations with different sets of kinetic profiles within the errorbars of the Thomson scattering measurements. Other sources of error, as the uncertainties in the measurement of the injected power, have not been taken into account. The values of such I_{NBCD} are roughly four times the experimental ones. In order to have an estimate of the relaxation time, this has been calculated for shot #24000 giving $\tau_{LR} = 57 \pm 46$ms.

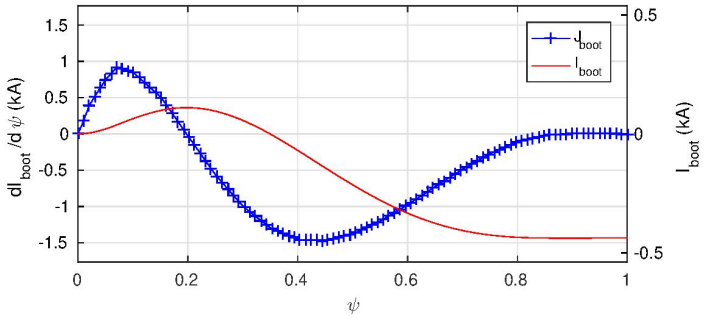

FIG. 10: Bootstrap-current density profiles and integrated current as a function of the normalized toroidal flux.

TABLE 1. VALUES OF THE NBCD, BOOTSTRAP (BS), COMPUTED NET CURRENT (COM) AND FITTED EXPERIMENTAL CURRENTS

Discharge	I_{NBCD}(kA)	I_{BS}(kA)	$I_{COM}=I_{NBCD}+I_{BS}$	I_{EXP}(kA)
#24000	+8,3±1,8	-0,4	+7,9±1,8	1,9±0,7
#25621	+5,9±1,3	+0,0	+5,9±1,3	1,7±0,1

6. DISCUSSION

Several uncertainties, both on the theoretical and on the experimental side may cause the large differences seen between the experimental results and the theoretical predictions. As it was explained in the introduction, the slowing-down simulations do not include CX losses, which are known to have a strong impact on the energy transferred from fast ions to the thermal plasmas. In principle, a reduction in the steady-state fast-ion density, especially in low-medium density plasmas, that could even reach a 50% of the fast ions' initial power, is expected and in this case, theoretical current would be significantly reduced. However, a reliable calculation of CX losses also needs an estimation of the neutral species profiles inside the plasma, which is not available at this time . Another potentially important source of error comes from the uncertainties in the determination of Z_{eff}. From Fig. 8, one can notice that the value of Z_{eff} has an impact on the shielding factor A_s. In this study, a flat profile of Z_{eff}=1.5 has been used, following radiation data analysis and modelling results obtained in similar shots [14]. Any deviation from the chosen Z_{eff} value will change the calculated current result. In particular, for lower Z_{eff} values, the shielding efficiency of plasma electrons is higher, meaning a lower level of NBCD. Of course, the impact of Z_{eff} variations on fast-ion slowing-down distribution must also be addressed to complete the picture. The determination of the available NBI power needs also assessment, since only port-through power is actually measured and the available power (and its corresponding shine through) are calculated by BBNBI. Having a calibrated measurement of the shine-through power may also help to narrow the indeterminacy in the results. Last but not least, the impact of AEs on the fast-ion confinement (which in tokamaks have shown to reduce the beam heating and current efficiency [15]) is not considered in the simulations although NBI in TJ-II always comes accompanied with AEs excitation. Finally, the difference between the vacuum magnetic equilibrium used for the simulations and the actual one, which is modified by the presence of all the sources of currents, NBCD mostly, must be also evaluated and its impact on the NBCD result determined by means of self-consistent simulations.

ACKNOWLEDGEMENTS

This work has been carried out within the framework of the EUROfusion Consortium and has received funding from the Euratom research and training programme 2014-2018 and 2019-2020 under grant agreement No 633053. The views and opinions expressed herein do not necessarily reflect those of the European Commission. This research was supported in part by project Y2018/NMT4750, Ministerio de Ciencia, Innovación y Universidades, Spain

REFERENCES

[1] McCARTHY, K. J., ET AL., A spectrally resolved motional Stark effect diagnostic for the TJ-II stellarator, Contrib. Plasma Phys. 55 (2015) 459-469

[2] VARJE, J. ET AL., High-performance orbit-following code ASCOT5 for Monte Carlo simulations in fusion plasmas, Submitted to Comput. Phys. Comm. (2019) (arXiv:1908.02482v1)

[3] NAKAJIMA, N., OKAMOTO, M., Beam-driven currents in the 1/vregime in a helical system, J. Phys. Soc. Japan 59 (1990) 3595-3601

[4] WATANABE, K. ET AL., Study on time evolution of toroidal current in LHD, J. Plasma Fusion Res. 5 (2002) 124-130

[5] NEUNER, U. ET AL., Measurements of the parameter dependencies of the bootstrap current in the W-7X stellarator, Nucl. Fusion 61 (2021) 036024

[6] SCHMITT, J. C. ET AL., Modeling, measurement and 3D equilibrium reconstruction of the bootstrap current in the Helically Symmetric Experiment, Physics of Plasmas 21 (2014) 092518

[7] LISTER, G., FAFNER: a fully 3D neutral beam injection code using Monte Carlo methods, Max-Planck-Institut für Plasmaphysik Technical Report IPP 4 (1985) 222

[8] LINIERS, M., ET AL., Beam transmission dependence on beam parameters for TJ-II Neutral Beam Injectors, Fusion Eng. Des. (2017) 259-262

[9] ASUNTA, O. ET AL., Modelling neutral beam injection in fusion devices: beamlet-based model for fast particle simulations, Comput. Phys. Comm. 188 (2015) 33-46

[10] FONTDECABA, J.M. ET AL., Comparisons of electron temperature and density, and ion temperature profiles in TJ-II the stellarator, Plasma Fusion Res., 5, (2010) S:2085

[11] HAPPEL, T. ET AL., Doppler reflectometer system in the stellarator TJ-II, Rev. Sci. Instrum. 80 (2009) 073502

[12] ESTRADA, T. ET AL., Turbulence and perpendicular plasma flow asymmetries measured at TJ-II plasmas, Nucl. Fusion 59 (2019) 076021

[13] VELASCO J.L. ET AL., Calculation of the bootstrap current profile for the TJ-II stellarator, Plasma Phys. Control. Fusion 53 (2011) 11

[14] CAPPA, Á., ET AL., 45th EPS Conf. on Plasma Phys. (2018) P4.1040

[15] GORELENKOV, N. N. ET AL., Energetic particle physics in fusion research in preparation for burning plasma experiments, Nucl. Fusion **54** (2014) 125001